JOURNAL OF VIROLOGY, Jan. 1997, p. 705–714 Vol. 71, No. 1
0022-538X/97/$04.00+0

Expression of Aleutian Mink Disease Parvovirus Capsid Proteins in Defined Segments: Localization of Immunoreactive Sites and Neutralizing Epitopes to Specific Regions

MARSHALL E. BLOOM,[1]* DAVID A. MARTIN,[1] KATRINA L. OIE,[1] MARK E. HUHTANEN,[1] FREDERICK COSTELLO,[1] JAMES B. WOLFINBARGER,[1] STANLEY F. HAYES,[2] AND MAVIS AGBANDJE-MCKENNA[3]

Laboratory of Persistent Viral Diseases[1] and Rocky Mountain Microscopy Branch,[2] Rocky Mountain Laboratories, National Institute of Allergy and Infectious Disease, Hamilton, Montana 59840, and Department of Biological Sciences, University of Warwick, Coventry CV4 7AL, England[3]

Received 30 July 1996/Accepted 10 October 1996

The capsid proteins of the ADV-G isolate of Aleutian mink disease parvovirus (ADV) were expressed in 10 nonoverlapping segments as fusions with maltose-binding protein in pMAL-C2 (pVP1, pVP2a through pVP2i). The constructs were designed to capture the VP1 unique sequence and the portions analogous to the four variable surface loops of canine parvovirus (CPV) in individual fragments (pVP2b, pVP2d, pVP2e, and pVP2g, respectively). The panel of fusion proteins was immunoblotted with sera from mink infected with ADV. Seropositive mink infected with either ADV-TR, ADV-Utah, or ADV-Pullman reacted preferentially against certain segments, regardless of mink genotype or virus inoculum. The most consistently immunoreactive regions were pVP2g, pVP2e, and pVP2f, the segments that encompassed the analogs of CPV surface loops 3 and 4. The VP1 unique region was also consistently immunoreactive. These findings indicated that infected mink recognize linear epitopes that localized to certain regions of the capsid protein sequence. The segment containing the hypervariable region (pVP2d), corresponding to CPV loop 2, was also expressed from ADV-Utah. An anti-ADV-G monoclonal antibody and a rabbit anti-ADV-G capsid antibody reacted exclusively with the ADV-G pVP2d segment but not with the corresponding segment from ADV-Utah. Mink infected with ADV-TR or ADV-Utah also preferentially reacted with the pVP2d sequence characteristic of that virus. These results suggested that the loop 2 region may contain a type-specific linear epitope and that the epitope may also be specifically recognized by infected mink. Heterologous antisera were prepared against the VP1 unique region and the four segments capturing the variable surface loops of CPV. The antisera against the proteins containing loop 3 or loop 4, as well as the anticapsid antibody, neutralized ADV-G infectivity in vitro and bound to capsids in immune electron microscopy. These results suggested that regions of the ADV capsid proteins corresponding to surface loops 3 and 4 of CPV contain linear epitopes that are located on the external surface of the ADV capsid. Furthermore, these linear epitopes contain neutralizing determinants. Computer comparisons with the CPV crystal structure suggest that these sequences may be adjacent to the threefold axis of symmetry of the viral particle.

Antibodies against the capsid proteins of Aleutian mink disease parvovirus (ADV) are a prominent feature in the immunopathogenesis of Aleutian mink disease (1–3, 16, 18). This infection is characterized by polyclonal hypergammaglobulinemia, plasmacytosis, immune complex glomerulonephritis, and interstitial nephritis (14, 38, 39). Antiviral antibodies commonly reach titers in excess of $1/10^6$ and can constitute over one-half of the gamma globulins (1–3, 43). Gamma globulins can comprise up to 50% of the total serum proteins (1–3), and in some instances, mink develop a gamma globulin pattern that exhibits evidence of restricted heterogeneity or monoclonality (2, 8, 42).

In spite of this pronounced antibody response, virus is not cleared and complexes of virus and antibody retain infectivity in vivo (14, 38, 40). Furthermore, the infectivity of ADV for macrophage target cells in vitro is dependent on antiviral antibodies (29, 30). In contrast, antiviral antibodies are capable of neutralizing ADV infectivity for Crandell feline kidney (CRFK) cells (29, 54). It is unknown if the same viral epitopes are involved in neutralization of infectivity for CRFK cells and the antibody-dependent enhancement of infectivity for macrophages.

A significant fraction of the anti-ADV antibody is directed against linear viral epitopes because antiviral antibody can be detected by immunoblotting at high serum dilutions (2). However, it is probable that there are also conformational epitopes, because a number of anti-ADV monoclonal antibodies react against intact virions but fail to react by immunoblotting against the denatured virion proteins (44).

ADV has two capsid proteins, VP1 and VP2, that derive from a single spliced mRNA (9, 14, 22, 23, 59). Transcription of this mRNA (R3) initiates at a 36-map-unit promoter, and the coding sequences encompass virtually the entire large right open reading frame. VP2, 647 amino acid residues in length, is the most abundant species in preparations of purified virions (90%) and has a molecular mass of 75 kDa. The 85-kDa VP1, which arises by alternate initiation on R3, has an additional 42 residues appended to the amino end of VP2 (Fig. 1). Although sera from virtually all infected mink react against both VP1 and VP2 (1–3, 18), it is unknown whether the antigenic sites

* Corresponding author. Mailing address: Laboratory of Persistent Viral Diseases, Rocky Mountain Laboratories, National Institute of Allergy and Infectious Disease, Hamilton, MT 59840. Phone: (406) 363-9275. Fax: (406) 363-9204. E-mail: mbloom@nih.gov.

(A)

```
                    10        20        30        40
                     *         *         *         *
ADV-G  VP1   MSKIPQHYPGKKRSAPRHVFIQQAKKKKQTNPAVYHGEDTIE
```

(B)

```
                    a         10        20        30        40        b         60        70        80        90        100       110       120       130       c         150
                    |          *         *         *         *        |          *         *         *         *         *         *         *         *        |          *
ADV-G  VP2   MDSTEAEQMDTEQATNQTAEAGGGGGGGGGGGGGGGGGVGNSTGGFNNTTEFKVINNEVYITCHATRMVHINQADTDEYLIFNAGRTTDTKTHQQKLNLEFFVYDDFHQQVMTPWYIVDSNAWGVWMSPKDFQQMKTLCSEISLVTLEQEI
ADV-TR VP2   ...A.P.....---------.....................................................................F.....................................
ADV-UT VP2   ...A.P.....................S.....................................................D.....A.K.....................F.....................................
ADV-PU VP2   ...A.P.....----------.....................................................................A.P.....................FM....................................

                    160       170       180       190       200       d         220       230       240       250       260       270       280       290       e         300
                     *         *         *         *         *        |          *         *         *         *         *         *         *         *        |          *
ADV-G  VP2   DNVTIKTVTETNQGNASTKQFNNDLTASLQVALDTNNILPYTPAAPLGETLGFVPWRATKPTQYRYYHPCYIYNRYPNIQKVATETLTWDAVQDDYLSVDEQYFNFITIENNIPINILRTGDNFHTGLYEFNSKPCKLTLSYQSTRCLGL
ADV-TR VP2   ..........................................................................................................I...K.....................
ADV-UT VP2   ..........................................................MGQ.Q.E.TGT.....................................................................
ADV-PU VP2   ................TV..Y.....................................................A.QSP.E.TGT.....................................S.I...K.....................

                    310       320       330       340       350       f         370       380       390       400       410       420       g         440       450
                     *         *         *         *         *        |          *         *         *         *         *         *        |          *         *
ADV-G  VP2   PPLCKPKTDTTHKVTSKENGADLIYIQGQDNTRLGHFWGEERGKKNAEMNRIRPYNIGYQYPEWIIPAGLQGSYFAGGPRQWSDTTKGAGTHSQHLQQNFSTRYIYDRNHGGDNEVDLLDGIPIHERSNYYSDNEIEQHTAKQPKLRTPP
ADV-TR VP2   ........................E.....................V.....................Q.....................N.....................
ADV-UT VP2   ........................E.....................V.....................Q.....................H.....................
ADV-PU VP2   .........V.....L...GEIT..E.................RN.....V.....................Q.....................H......T.....H...

                    460       470       480       490       500       510       520       h         530       540       550       560       570       580       i         600
                     *         *         *         *         *         *         *        |          *         *         *         *         *         *        |          *
ADV-G  VP2   IHHSKIDSWEEEGWPAASGTHFEDEVIYLDYFNFSGEQELNFPHEVLDDAAQMKKLLNSYQPTVAQDNVGPVYPWGQIWDKKPHMDHKPSMNNNAPFVCKNNPPGQLFVKLTENLTDTFNYDENPDRIKTYGYFTWRGKLVLKGKLSQVT
ADV-TR VP2   ..........................................D.....................D.....................
ADV-UT VP2   ..........................................E.....................D.....................
ADV-PU VP2   V..H.....................................N....E.....................GL.................DV.....S.....................

                    610       620       630       640
                     *         *         *         *
ADV-G  VP2   CWNPVKRELIGEPGVFTKDKYHKQIPNNKGNFEIGLQYGRSTIKYIY
ADV-TR VP2   ..................N.....................
ADV-UT VP2   ................S..N.....................
ADV-PU VP2   ................S..N.....................L.
```

FIG. 1. ADV capsid protein sequences and locations of expression construct segments. (A) The 42-amino-acid sequence of the unique VP1 region of ADV-G contained in pVP1. The exact VP1 sequence for other ADV isolates has not been determined. (B) The 647-amino-acid sequence of ADV-G VP2 aligned with the VP2 sequences of ADV-TR, ADV-Utah (ADV-UT), and ADV-Pullman (ADV-PU) isolates (28, 35). The boundaries of the sequence captured in the expression constructs pVP2a through pVP2i are indicated by vertical arrows and lowercase letters over the first residue of each segment. The regions corresponding to the variable surface loops 1 through 4 of CPV (21) were captured in pVP2b, pVP2d, pVP2e, and pVP2g, respectively, and are underlined. The ADV hypervariable region was contained in pVP2d (11, 12).

are uniformly distributed along the polypeptides or if viral epitopes are confined to certain regions of the proteins.

The topographic distribution of ADV antigens within the viral particle also remains to be determined. However, the three-dimensional configuration of the virion proteins within the capsid has been elucidated for several parvoviruses (6, 7, 21, 55), e.g., canine parvovirus (CPV) (55, 58), feline panleukopenia virus (5), and B19 parvovirus (4), using X-ray crystallographic analysis. Parvovirus capsids are typical icosahedral particles composed of 60 asymmetric protein subunits (protomers) (6, 7, 21, 55, 58). Each protomer is bounded by a fivefold and two threefold axes of symmetry, and a twofold axis of symmetry lies between the threefold axes. Several features of interest of the protein coat are (i) an eight-stranded antiparallel β barrel which is mostly internal and forms the shell of the virion, (ii) a spike at each of the threefold axes that is elevated above the mean radius of the particle, (iii) a depression on the twofold axes between the threefold axial spikes, and (iv) a canyon surrounding each fivefold axis. The surface of the particle is formed by segments of polypeptide inserted between the β strands. These insertions can be divided into four recognizable and distinct loops (loop 1 through loop 4) that are represented on the surface of the particle. Loop 3 and loop 4 of each promoter overlap and interdigitate with the analogous portions of two other polypeptides to form the threefold spike. The location within the capsid of the VP1 molecules, which comprise less than 10% of the total (24), has not been resolved (6, 21, 55, 58).

Computer alignments of the CPV capsid protein sequence with that of ADV make it possible to extrapolate certain features of the ADV capsid structure (11, 12, 21, 35). For example, the *Eco*RI-*Eco*R5 ADV segment that acts as a host range determinant for CRFK cells (12) aligns with surface loop 1 of CPV, which contains a host range determinant critical for growth in canine cells. In addition, the hypervariable region of the ADV capsid gene, found at map units 64 to 65 (12, 35), aligns well with surface loop 2 of CPV, a region which encompasses a CPV/FPV strain-specific epitope. The hypervariable region shows a remarkable number of sequence differences among ADV viral isolates; for example, 8 of 11 amino acids in this region differ between ADV-G and ADV-Utah (11, 28, 35). The linear alignment with CPV surface loops 3 and 4 is not as precise as that for loops 1 and 2 (12, 21); however, it is adequate to allow tentative assignment of ADV sequences to those loops, too.

Because of the unusual nature of the antiviral antibody response seen in ADV infections, we wanted to know if specific regions of the virion proteins were recognized by infected mink and if it might be possible to relate antigens to specific features of the particles. To study the distribution of antigenic regions on the ADV virion proteins, the entire ADV-G capsid protein gene was expressed as 10 nonoverlapping fusion proteins with maltose-binding protein (MBP) (10, 27, 34), denoted pVP1 and pVP2a through pVP2i. The segments were designed so that the regions tentatively corresponding to the four surface loops of CPV were captured in individual fragments. In addition, the portions corresponding to CPV surface loop 1 (pVP2b) and surface loop 2 (pVP2d containing the ADV hypervariable region) from ADV-Utah were also prepared.

MATERIALS AND METHODS

Construction of ADV capsid protein expression plasmids. The ADV-specific segments, except that for pVP2a, were prepared as in-frame *Eco*RI-*Sal*I fragments from a VP1/VP2 ADV-G cDNA (9, 23) by PCR amplification (35, 48) utilizing primers that incorporated the restriction site as well as a downstream termination codon. Fragments corresponding to VP2b and VP2d were also amplified in an identical fashion from a genomic clone of ADV-Utah (11, 35). The amplification products were treated with proteinase K (25) and digested with *Eco*RI and *Sal*I. They were subsequently ligated into *Eco*RI-*Sal*I-digested pMAL-c2 in frame with MBP prior to transformation into *Escherichia coli* JM109 (10, 27, 34, 36, 60).

pVP2a, the amino-terminal portion of VP2 (9, 11), contained a long stretch of glycine residues that were deleted during PCR amplification. Consequently, the VP2a insert was derived by first cloning a large portion of VP2 (a blunt-ended *Xcm*I-*Hin*dIII fragment) into *Xmn*I-*Hin*dIII-digested pMAL-c2 and subsequently deleting the ADV *Eco*RI-*Hin*dIII portion to generate pVP2a.

The actual sequences of the ADV-specific VP2 protein segments of ADV-G are shown in Fig. 1 and compared with the corresponding regions of other ADV isolates, ADV-TR, ADV-Utah, and ADV-Pullman (28, 35). The locations of the four CPV surface loops, embedded in segments pVP2b, pVP2d, pVP2e, and pVP2g, are underlined (12, 21).

Colonies positive for ADV by colony hybridization were propagated in 2-ml broth cultures, and 1-ml aliquots were treated with 1 mM isopropythiogalactopyranoside (IPTG) for 90 min in order to induce fusion proteins under the control of the pMAL-c2 *tac* promoter (10, 27, 34). Cell pellets were lysed in Laemmli sample buffer and analyzed by sodium dodecyl sulfate-polyacrylamide gel electrophoresis (SDS-PAGE) (18). Clones expressing inducible fusion proteins of the expected size were selected for further work. The structures of all constructs were confirmed by sequencing purified plasmid DNA prepared from clones of interest (11, 12, 35).

For batch preparations of recombinant proteins, 100- to 500-ml broth cultures were grown at 37°C to an optical density at 450 nm of 0.5 and induced with 1 mM IPTG for 90 min. Cell pellets were lysed, and the MBP-ADV fusion proteins were captured by affinity chromatography on amylose resin columns and subsequently eluted with 10 mM maltose (27, 34). Fractions containing the purified fusion proteins were identified by SDS-PAGE, pooled, concentrated by dialysis against dry Sephadex G-50, and stored at −20°C. Final protein concentrations were determined by using the Bradford assay (Bio-Rad).

Viruses, cells, and sera. The ADV-G isolate of ADV was propagated in CRFK cells as described previously (17).

Pooled terminal sera from mink infected with either ADV-TR, ADV-Pullman, or ADV-Utah (28, 35) were used (Fig. 2). To minimize background in immunoblots, sera were absorbed with boiled lysates of pMAL-c2-transformed bacteria induced with IPTG. Individual sera were collected from sapphire (Aleutian) and pastel (non-Aleutian) mink approximately 60 days after mock infection or intraperitoneal infection with $>10^7$ mink 50% infectious doses (ID_{50}) of ADV-TR, 10^7 mink ID_{50} of ADV-Utah, 10^6 mink ID_{50} of ADV-Pullman, or 10^7 fluorescence-forming units of the cell culture ADV-G strain. Other studies describing the results of infection of these mink have been reported (28, 35).

Heterologous antisera were prepared against purified ADV-MBP fusion proteins by injecting rabbits with 0.1 mg of the recombinant proteins emulsified in Freund's complete adjuvant. Booster injections were prepared in Freund's incomplete adjuvant and given at monthly intervals. Another antiserum was prepared by similarly inoculating rabbits with ADV-G capsids, purified from Sf9 cells infected with the recombinant baculovirus Ac-ADV-1 (59). The presence of anti-ADV capsid antibodies was assayed by immunoblotting against lysates of ADV-G-infected CRFK cells (13). The anti-ADV monoclonal antibody Y-2-9 is active in immunoblotting against both capsid proteins. An anti-rabies virus monoclonal antibody (355), graciously provided by Donald Lodmell, served as a negative control.

SDS-PAGE and immunoblotting. Lysates of bacterial cultures or purified ADV-MBP fusion proteins were subjected to SDS-PAGE (10% gel) in a Bio-Rad Mini-PROTEAN II mini-slab gel apparatus. For some applications, Coomassie blue was incorporated into the upper running buffer so that staining and identification of proteins were possible during electrophoresis (51). Proteins stained in this way could be successfully transferred to the membranes but were unreactive with antibody.

Proteins in the minigels were subsequently electroblotted onto Hybond-C Extra membranes as reported previously (3, 12). The membranes were blocked overnight in phosphate-buffered saline (PBS)–0.5% Tween 20 (PBS-T) containing 10% fish gelatin (Hipure liquid gelatin; Norland Products Inc., New Brunswick, N.J.) (32, 49). After washing, the membranes were reacted at room temperature for 2 h with the various sera, diluted 1/1,000 (mink sera) or 1/100 (rabbit sera) in PBS-T. Monoclonal antibody supernatants were used undiluted. Following washing in PBS-T, the membranes were incubated with a 1:5,000 dilution of horseradish peroxidase-conjugated protein A for 1 h. After a final washing, a chemiluminescence signal was developed by using either the ECL system (Amersham) or the Renaissance system (Dupont-NEN) (56).

Immunoblotting of lysates of uninfected CRFK cells or CRFK cells infected with ADV-G was performed on SDS–7.5% polyacrylamide gels as previously noted, using a chemiluminescent reporter system (56).

Anti-ADV antibody determinations. Serum antibody to ADV was detected by counterimmunoelectrophoresis (16, 35).

For detection of in vitro neutralizing antibody (29, 54), fourfold dilutions of sera (beginning with a 1/50 dilution) or monoclonal antibodies (beginning with undiluted supernatant) were prepared in a 96-well tray, using medium as the diluent. Equal volumes (75 μl) of a 1/20 dilution of ADV-G that had been freshly ether extracted were added to the same wells and incubated at 37°C for 1 h after

mixing. Antibody-virus mixtures were added to wells of a flat-bottomed 96-well tray that had been seeded the previous day with 1.5×10^4 CRFK cells. Following incubation at 31.8°C for 72 h, the monolayers were washed once with PBS, fixed with a fresh solution of 80% acetone in PBS at room temperature for 20 min, and stained for 1 h at room temperature with a direct fluorescein isothiocyanate-conjugated immunoglobulin G (IgG) preparation from ADV-infected mink sera. After washing and addition of 20 to 50 μl of 90% glycerol in PBS, the preparations were examined by epifluorescence microscopy using a 10× objective and a 10× ocular lens with the trays inverted on the stage. Any serum dilution in which fewer than 30% ADV-positive cells (>70% reduction compared to virus alone) remained was considered to be positive for neutralizing activity. All samples were assayed in duplicate.

Immune electron microscopy (IEM). Virions were partially purified from lysates of ADV-G-infected CRFK cells that had been freeze-thawed and sonicated. After clarification and extraction of lipids with chloroform, virus-containing suspensions were layered over 40% sucrose in PBS and ultracentrifuged at 25,000 rpm overnight at 4°C in a Beckman SW41 rotor (Beckman Instruments, Fullerton, Calif.) (23, 59). The pellets were resuspended in PBS by sonication and passed through a 100-nm-pore-size filter to minimize virus aggregates. An identical procedure was used to obtain self-assembled empty capsids from Sf9 cells infected with the recombinant baculovirus Ac-ADV-1 (23, 59).

Virions, diluted 1/10 (ADV-G virions) or 1/1,000 (Ac-ADV-1 capsids) in 0.25 M ammonium acetate–0.002 M EDTA, were adsorbed for 30 min at ambient temperature onto 400-mesh copper grids freshly coated with 2.8% Parlodion. The grids were blocked by inversion onto a drop of PBS containing 3% bovine serum albumin (PBS-BSA) for 15 min and then incubated for 2 h on a drop of test serum diluted in 1:100 in PBS-BSA and filtered immediately prior to use. After washing in distilled water and reblocking in PBS-BSA, the specimens were incubated on a drop of goat anti-rabbit IgG labeled with 5-nm gold particles (1:20 dilution; Ted Pella, Redding, Calif.). After sequential washing in PBS and distilled water, the samples were stained with 0.3% uranyl acetate and photographed at a screen magnification of ×86,000 in a Hitachi HU-11E1 electron microscope (Hitachi Instruments, Mountain View, Calif.).

A minimum of 50 virus particles were observed for each serum tested. Samples in which the 25 nm capsids were consistently decorated with the 5-nm electron-dense gold particles were scored as positive by a blinded observer.

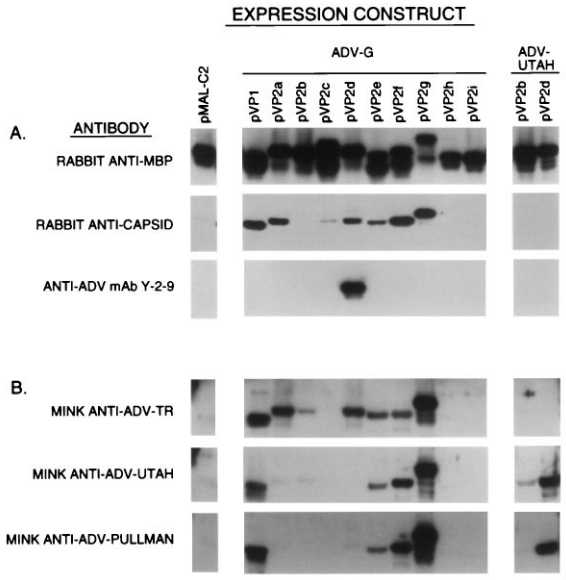

FIG. 2. Immunoblot analysis of ADV capsid-MBP fusion proteins. Fusion proteins were purified from bacteria containing either pMAL-C2 (10, 34) or the indicated ADV expression constructs. One microgram of each of the proteins was subjected to SDS-PAGE (10% gel) and transferred onto Hybond-C Extra membranes prior to immunoblotting. Replicate membranes were reacted with the following antisera: rabbit anti-MBP, rabbit anti-ADV-G capsid, and murine anti-ADV-G capsid monoclonal antibody (MAb) Y-2-9 (A) and pooled sera from mink infected with either ADV-TR, ADV-Utah, or ADV-Pullman (B) (28, 35). Antibody was detected by using horseradish peroxidase-conjugated protein A, and the signal was developed with chemiluminescence (56).

RESULTS

Reactivity of heterologous antisera and monoclonal antibodies to segments of ADV capsid proteins. After determining that the capsid protein clones expressed inducible MBP fusion proteins of the proper sizes, we proceeded to examine the antigenic nature of the proteins. The fusion proteins were purified on amylose columns (27, 34) and reacted by immunoblotting with a serum directed against MBP (Fig. 2A). A strong reaction was noted with all clones, indicating that the fusion proteins all retained MBP antigenic determinants. This serum did not recognize ADV capsid proteins (data not shown).

We used the fusion protein panel to map the epitope for anti-ADV-G monoclonal antibody Y-2-9, which recognizes both VP1 and VP2 in immunoblot assay. The Y-2-9 antibody reacted only with the ADV-6 VP2d sequence and not the corresponding sequence in ADV-Utah (Fig. 2A). Thus, the linear epitope for this monoclonal antibody maps to the putative homolog of CPV surface loop 2 and is specific for an ADV-G-like sequence (21, 35).

A rabbit antiserum raised against intact ADV-G capsids expressed by a recombinant baculovirus (Ac-ADV-1) (59) reacted with some but not all of the segments (Fig. 2A). In particular, reactions were noted against the VP1 unique sequence (pVP1), the amino terminus of VP2 (pVP2a), and also segments pVP2d, pVP2e, pVP2f, and pVP2g. As was found for Y-2-9, the polyclonal serum reacted only against ADV-G pVP2d fragment and not the corresponding sequence from ADV-Utah (pVP2d-Utah). The serum was prepared against ADV-G capsids; thus, the fact that not all segments were reactive indicated that not all regions of the capsid protein contained linear epitopes.

These results showed that the set of fusion proteins was a suitable panel for analyzing serum reactivities against linear viral epitopes. Furthermore, they also suggested that a type-specific linear epitope might be located in the pVP2d segment, the hypervariable portion of the ADV capsid protein containing surface loop 2 of CPV (21, 26, 35).

Reactivity of ADV-infected mink sera to segments of ADV capsid proteins. The panel of fusion proteins was reacted against pooled terminal sera from mink infected with either ADV-TR, ADV-Utah, or ADV-Pullman (Fig. 2B) (28, 35). All of the serum pools reacted strongly with pVP2g (loop 4), pVP1 (VP1 unique), and pVP2f and pVP2e (loop 3) in roughly descending order of intensity. Despite the fact that the three in vivo ADV isolates have conserved differences from ADV-G in the sequences contained in pVP2e, pVP2f, and pVP2g (26, 35), no difference in reactivity was evident. This finding suggested that the sequence variation in these portions of the capsid gene does not define unique antigenic differences among the virus isolates.

This finding was in sharp contrast to the results with pVP2d, the segment containing the hypervariable region (Fig. 2B) (11, 12). The ADV-TR serum pool reacted with the ADV-G pVP2d but not the ADV-Utah sequence. ADV-TR and ADV-G have identical hypervariable region amino acid sequences (Fig. 1B) (35). On the other hand, the ADV-Utah and ADV-Pullman serum pools reacted strongly with the ADV-Utah segment but very faintly with the ADV-G pVP2d. Consequently, this finding strongly inferred that the type-specific epitope identified in pVP2d by the rabbit serum and the monoclonal antibody also was recognized by infected mink.

The ADV-TR serum pool reacted strongly with pVP2a, whereas the ADV-Utah and ADV-Pullman pools were barely above background. Two residues in the pVP2a segment are conserved among the in vivo isolates, and it is possible that the differences define an antigen not present in ADV-G (Fig. 1B).

The pVP2b segment contains both a host range determinant for permissive growth of ADV in CRFK cells and the portion

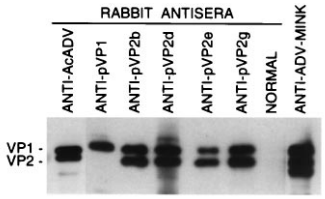

FIG. 3. Immunoblot analysis of heterologous antisera prepared against ADV capsid-MBP fusion proteins. Rabbit antisera were prepared against purified ADV capsid-MBP fusion proteins corresponding to the VP1 unique region (pVP1) and the four constructions analogous to the variable surface loops 1 through 4 of CPV, pVP2b, pVP2d, pVP2e, and pVP2g, respectively (21). These sera, along with a heterologous anti-ADV-G capsid serum, normal rabbit serum, and ADV-infected mink serum, were tested by immunoblotting at a 1/100 dilution against lysates of ADV-G-infected CRFK cells. Antibody was detected by using horseradish peroxidase-conjugated protein A, and the signal was developed with chemiluminescence (56).

of the capsid gene aligning with CPV surface loop 1 (12, 21). The ADV-TR sequence is similar to the ADV-G sequence and differs from those of ADV-Utah and ADV-Pullman (Fig. 1B) (35). The ADV-TR pool reacted well with the ADV-G pVP2b but weakly with the ADV-Utah sequence, whereas the ADV-Utah serum pool showed the opposite reactivities.

Several segments were unreactive. None of the sera reacted with pVP2c, although the ADV-Utah and ADV-TR sequences are identical with the ADV-G sequence. The segments pVP2h and pVP2i were also unreactive with the serum pools; however, in this area, the sequences of ADV-Utah, ADV-TR, and ADV-Pullman have conserved differences from ADV-G. Consequently, it was not possible to determine if nonreactivity was due to antigenic differences or to a lack of linear epitopes in this region of the protein.

We extended these results by assaying the fusion protein panel against a number of individual terminal sera from trios of sapphire (Aleutian) and pastel (non-Aleutian) mink either mock infected or infected with several different isolates of ADV (28, 35). In brief, the findings confirmed those made with the serum pools.

A clear pattern of reactivity to the panel of fusion proteins was apparent among the mink inoculated with ADV-Utah, ADV-TR, or ADV-Pullman. Furthermore, the general pattern was the same regardless of virus inoculum or mink genotype. Sera from all of the mink (18 of 18) had antibodies against pVP2g, and the anti-pVP2g reactions were also invariably the strongest. The next most frequently recognized segment was the VP1 unique sequence, pVP1 (16 of 18 mink). More than 50% also reacted against pVP2e and pVP2f. All six of the ADV-TR-infected mink reacted with the ADV-G VP2d segment, whereas only two of six reacted weakly with the corresponding ADV-Utah portion. In contrast, all six of the ADV-Utah-infected mink reacted with the ADV-Utah VP2d, while four of six reacted weakly with the ADV-G segment. Although ADV-TR-infected mink were more likely to react against the pVP2b sequence, no preferential pattern was apparent with the ADV-Utah or ADV-Pullman sera. Constructs pVP2c, pVP2h, and pVP2i were rarely recognized by the mink sera. None of the mock-infected mink or those infected with the cell culture ADV-G had any evidence of disease, and their sera did not contain detectable antibody to ADV. None of these sera reacted against the panel of fusion proteins by immunoblotting. Thus, results from a number of individual mink infected with several strains of virus confirmed the findings from the serum pools that the linear epitopes were concentrated in certain regions of the capsid proteins.

Characterization of heterologous antisera directed against capsid protein segments. Rabbits were injected with affinity chromatography-purified fusion proteins from the VP1 unique and the ADV segments containing the analogs to the four surface loops of CPV (pVP2b, pVP2d, pVP2e, and pVP2g).

By immunoblot analysis, all of the rabbit sera reacted with capsid proteins in ADV-G-infected CRFK cell lysates (9, 14, 15, 18). The anti-VP1 unique serum recognized exclusively VP1, whereas the others reacted with both capsid proteins, VP1 and VP2 (Fig. 3). Thus, these segments were capable of inducing antibodies against the bona fide viral gene products.

To determine if any of these sera were capable of binding to virions, we performed IEM. Decoration of virus particles was readily observed with the antisera prepared against intact capsids, pVP2e (loop 3) and pVP2g (loop 4) (Table 1 and Fig. 4). The anti-pVP2g sera decorated the particles more densely. The rabbit sera prepared against pVP1 (the VP1 unique region), pVP2b (loop 1), and pVP2d (loop 2) were negative. The same results were obtained regardless of whether the virions were native ADV-G virions (15) or self-assembled capsids from Sf9 cells infected with the recombinant baculovirus Ac-ADV-1 (59).

The antibody preparations were also tested for the ability to neutralize ADV-G infectivity in CRFK cells (29, 54). Sera from ADV-infected mink contained high levels of neutralizing antibody, and the rabbit anti-capsid antibody also neutralized (Table 1). Of the rabbit sera prepared against the ADV segments, only the two directed against the proteins containing loop 3 (pVP2e) and loop 4 (pVP2g) contained detectable neutralizing antibody. The other sera, including the anti-VP1-spe-

TABLE 1. Characterization of antisera prepared against ADV virion protein-MBP fusion proteins[a]

Serum	Immunoblot[b]		Neutralization titer[c]	IEM[d]
	VP1	VP2		
Normal	−	−	<1/50	−
Anticapsid	+	+	1/50	+
Anti-pVP1 (VP1 unique)	+	−	<1/50	−
Anti-pVP2b (loop 1)	+	+	<1/50	−
Anti-pVP2d (loop 2)	+	+	<1/50	−
Anti-pVP2e (loop 3)	+	+	1/800	+
Anti-pVP2g (loop 4)	+	+	1/800	+
MAb control	−	−	<1/50	NT
Anti-ADV MAb Y-2-9	+	+	<1/50	NT
Normal mink	−	−	<1/50	NT
ADV-infected mink	+	+	1/3,200	NT

[a] Sera were characterized for reactivity in several assays. The sera included normal rabbit sera, rabbit antisera prepared against purified ADV virions expressed by the recombinant baculovirus AcADV-1, or rabbit antisera prepared against affinity-purified preparations of the indicated ADV virion protein-MBP fusion proteins. In addition, an anti-ADV-G and a control monoclonal antibody (MAb) were tested, as were serum pools from normal and ADV-infected mink. NT, not tested.

[b] Sera were tested by immunoblotting against lysates of ADV-G-infected CRFK cells for reactivity against VP1 and VP2 as detailed in the text. Rabbit sera were diluted 1/100, mink sera were diluted 1/1,000, and monoclonal antibodies were undiluted.

[c] Dilutions of sera were incubated with equal volumes of ADV-G at 37°C for 1 h. The mixtures were added to CRFK cells in a 96-well tray and incubated at 31.8°C for 72 h. The cultures were examined for residual ADV-infected cells as described in the text. Dilutions of sera exhibiting >70% reduction in number of ADV-positive cells were considered positive for neutralizing activity.

[d] The indicated rabbit sera were diluted 1:100 in PBS-BSA and incubated with ADV capsids adsorbed on copper grids. After washing, the grids were reacted with anti-rabbit IgG labeled with 5-nm gold particles. After washing and staining with 0.3% uranyl acetate, specimens were examined by IEM. A positive reaction was scored when the capsids were consistently decorated with the electron-dense gold particles. Details are provided in the text.

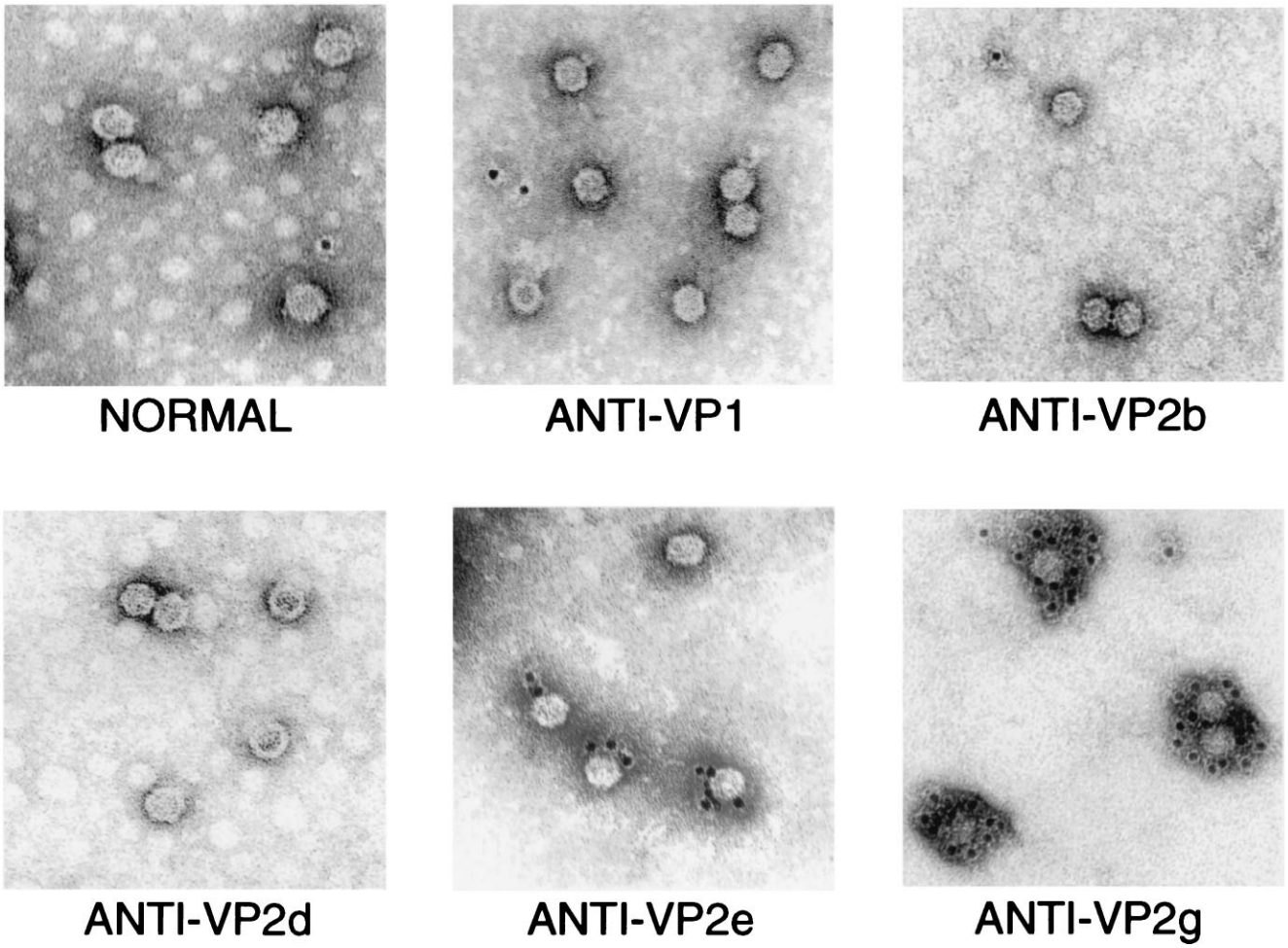

FIG. 4. IEM analysis of heterologous antisera prepared against ADV capsid-MBP fusion proteins. ADV-G capsids, purified from Sf9 cells infected with the recombinant baculovirus Ac-ADV-1 (59), were adsorbed onto grids and reacted with 1/100 dilutions of normal rabbit serum or the rabbit sera made against the purified fusion proteins from pVP1 (VP1 unique), pVP2b (loop 1), pVP2d (loop 2), pVP2e (loop 3), and pVP2g (loop 4). Samples were incubated with goat anti-rabbit IgG labeled with 5-nm gold particles and examined by electron microscopy. The binding of antibody to the capsids was revealed by the decoration of particles with the electron-dense gold particles. Although not depicted, antiserum against intact capsids also decorated the capsids.

cific and the anti-loop 2 (pVP2d) monoclonal antibody, Y-2-9, failed to neutralize infectivity for CRFK cells. Interestingly, none of the heterologous antisera nor monoclonal antibody Y-2-9 was positive in counterimmunoelectrophoresis.

DISCUSSION

We expressed the ADV capsid protein sequence in a panel of 10 nonoverlapping segments and examined several of their immunological properties. The design took into account information about the crystal structure of CPV and several other parvoviruses (6, 7, 21). Specifically, the regions likely to be analogous to the four polypeptide loops represented on the CPV particle surface were captured in separate expression constructions (12, 21, 35). Our findings clearly indicated that mink infected with ADV do not produce antibodies to all regions of the capsid proteins and that, therefore, linear viral epitopes are probably localized to specific areas of the proteins.

Several regions of the ADV capsid proteins were consistently immunoreactive with sera from seropositive ADV-infected mink. All animals showing evidence of infection had antibodies against pVP2g regardless of mink genotype, antibody titer, or virus inoculum. The reactions against pVP2g, in addition to being the most frequent, were also invariably the strongest. More than 50% of mink also reacted against pVP2e and pVP2f. In addition, heterologous antisera directed against pVP2e and pVP2g neutralized ADV-G infectivity for cell culture (Table 1) and decorated particles in IEM (Table 1 and Fig. 4). Linear alignment suggests that ADV pVP2e, pVP2f, and pVP2g tentatively correspond with the CPV linear sequence encompassing surface loops 3 and 4 (12, 21).

To relate our findings to the putative virion structure, we

FIG. 5. Proposed locations of variable surface loops on the capsid surface of ADV. A linear sequence alignment was performed between the VP2 amino acid sequences of ADV and CPV and was used to delineate the locations of several of the ADV VP2 segments corresponding to the segments of CPV. This information was used to project the ADV sequence onto the roadmap of one asymmetric unit of the capsid (20). Upper roadmap: pVP2b = blue, pVP2c = green, pVP2d = red. Lower roadmap: pVP2e = blue, pVP2f = green, pVP2g = red.

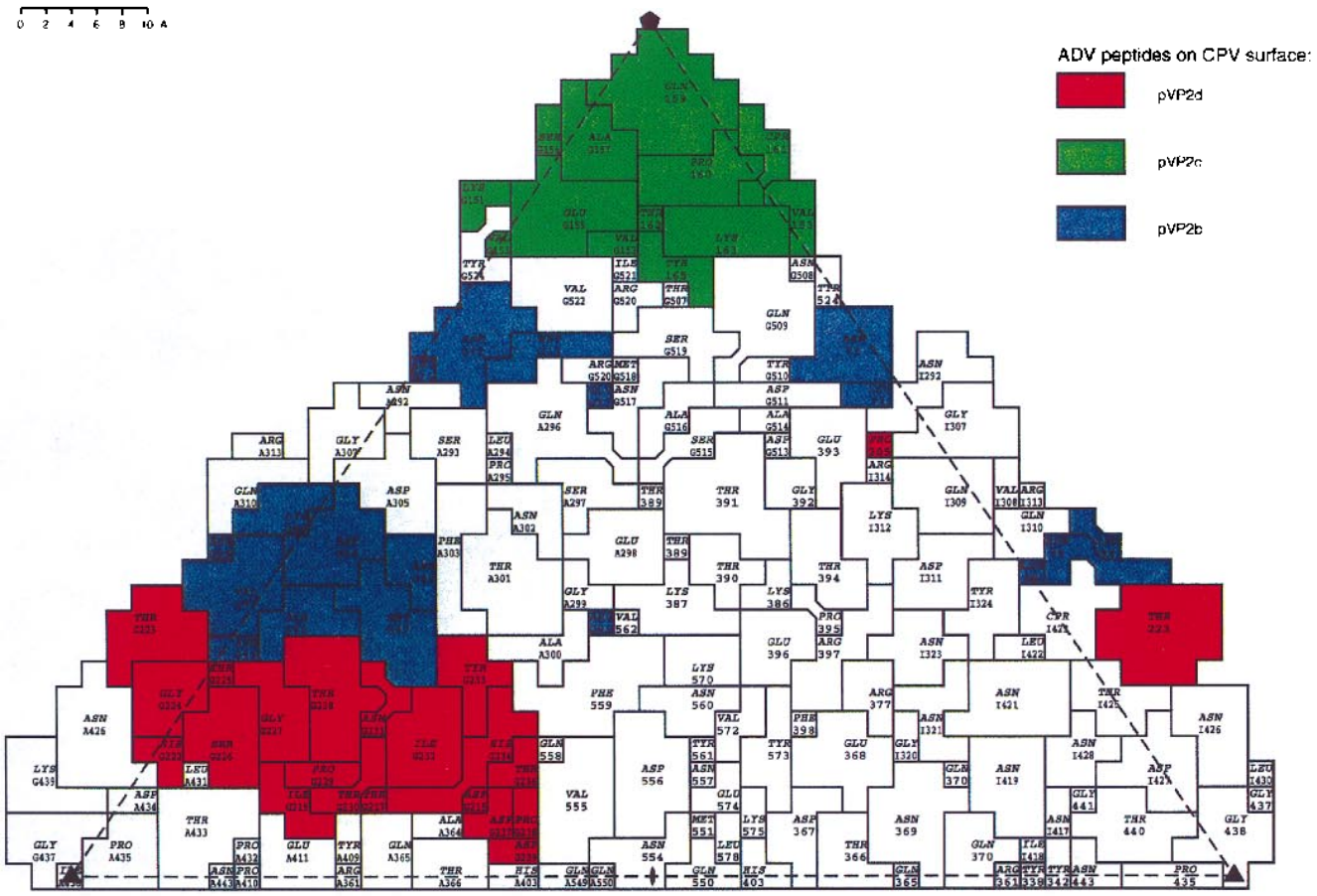
0 2 4 6 8 10 Å
ADV peptides on CPV surface:
pVP2d
pVP2c
pVP2b

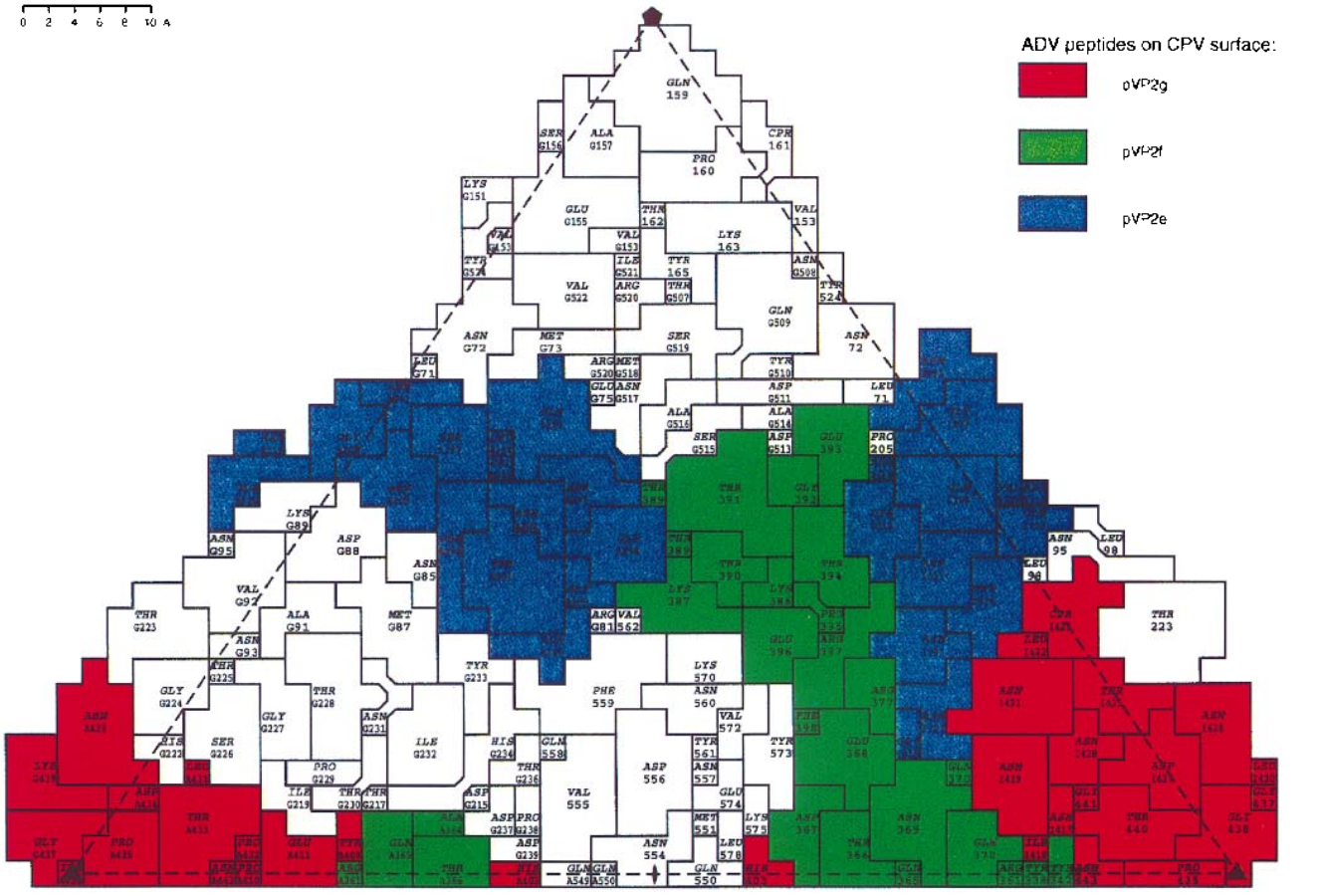
0 2 4 6 8 10 Å
ADV peptides on CPV surface:
pVP2g
pVP2f
pVP2e

constructed a roadmap of the ADV capsid surface based on the aligned amino acid sequences of ADV and CPV (Fig. 5) (6, 12, 20, 21, 58). Portions of segments pVP2e, pVP2f, and pVP2g on the capsid surface were localized to the elevated spike and shoulder contiguous with the threefold axis of symmetry, with pVP2g forming the apex of the spike. Of course, it must be noted that precise definition of the sequences forming the spike must await solution of the atomic structure of ADV. Nevertheless, the results, taken together, suggested that this region contains a major ADV linear epitope, which is located on the exterior of the viral particle and is a target for neutralizing antibody.

The area around the threefold spike of the capsid has been implicated as a major antigenic domain of other parvoviruses (6, 7, 21, 55, 58), and there are both linear and conformational epitopes (6, 19, 31, 33, 45, 50, 55). One major CPV epitope on the threefold spike is specified by the interaction of loops 1, 2 and 4, and another on the shoulder of the threefold spike has residues from both loop 1 and loop 4 (6, 7). Consequently, assignment of reactivity to specific linear sequences is difficult because of this interaction of noncontiguous residues. Nevertheless, epitope mapping studies on CPV identify neutralizing epitopes to loops 3 and 4 (21, 55). In fact, analysis of CPV mutants escaping neutralizing monoclonal antibodies (55) clearly places at least two neutralizing determinants on the threefold pike region. Therefore, our results suggested that some of the neutralizing epitopes of ADV may be similarly localized to loops 3 and 4.

The 42-amino-acid VP1 unique sequence (pVP1) (9) was recognized by the majority of infected mink, indicating that epitopes on this polypeptide are regularly antigenic during the course of ADV infection. However, the monospecific anti-VP1 antibody did not decorate purified virions or neutralize infectivity in vitro. Fewer than 10% of the 60 capsid proteins in each virion are VP1, which translates to fewer than six copies of the 42-amino-acid sequence per particle (24). The precise location of VP1 in CPV virions has not been elucidated, although most of the VP1 sequences are probably internal (21, 58). CPV epitope mapping studies identifies antigenic sites on VP1, and there may also be T-cell epitopes in this region (31, 33, 46, 57). Furthermore, for the human parvovirus B19, antibodies to the VP1 region also have potent neutralizing activity, and the VP1 sequence can be demonstrated on the surface of the particle (47, 53). These differing results may be partly due to the fact that the B19 and CPV VP1 sequences are long (229 and 143 amino acid residues, respectively) (52, 57), whereas that of ADV is much shorter (42 amino acids) (9, 37). Alternatively, the portion of the ADV VP1 unique domain recognized by our antibody may reside internally or in a depression on the virion which is inaccessible to antibody molecules (6, 7, 21, 58).

Computer alignment indicates that the 11-amino-acid hypervariable region of the ADV VP2 captured in pVP2d aligns with the exposed residues of CPV surface loop 2, another region implicated in CPV antigenicity (11, 12, 21). The anti-ADV-G monoclonal antibody Y-2-9 and the rabbit anti-ADV-G capsid serum reacted exclusively with the ADV-G VP2d segment but not with the corresponding segment from the ADV-Utah sequence (Fig. 2A). Furthermore, although the results were not as clearcut, sera from mink infected with a particular virus isolate showed preferential reactivity with the isotypic VP2d sequence (Fig. 2B). The apparent cross-reactivity that was observed might indicate other epitopes in this fragment outside the actual hypervariable region or might be due to the fact that in vivo-derived isolates of ADV often are mixtures of viruses (26). Nevertheless, the results considered together strongly suggested that the hypervariable region contains a type-specific ADV linear epitope for mink.

In spite of the possibility that pVP2d, the ADV homolog for surface loop 2 (21, 58), was implicated as a linear antigenic determinant, the rabbit antiserum to pVP2d did not neutralize ADV-G infectivity or decorate particles by IEM. The pVP2d sequence also had residues on the capsid surface (Fig. 5). In fact, superimposition of specific ADV residues on the CPV roadmap predicted that the hypervariable region residues Q----WTGT are surface residues on the shoulder of the threefold spike overlaying CPV residues T223----S226, G227, T228, P229 (12, 21). Interestingly, the Q-----TGT motif is conserved between the ADV-Utah and ADV-Pullman sequences (35), and sera from mink infected with these isolates reacted preferentially against the ADV-Utah construction. If these few amino acids are in fact part of the linear epitope in this segment, there may be insufficient representation of the sequence on the viral surface to mediate antibody binding or neutralization. On the other hand, failure to mediate in vitro neutralization and IEM might also mean that the epitopes in this segment are simply not accessible to antibody for steric reasons (6). Alternatively, perhaps these residues are also part of an epitope composed of noncontiguous residues similar to those alluded to previously for CPV in which several loops interact (6, 7).

Segments pVP2b (analog of CPV surface loop 1) and pVP2c also have regions that can be tentatively mapped onto the capsid surface. In fact, CPV VP2 residue 93, aligning with ADV VP2 residue Q94 (present in pVP2b), is implicated in CPV host range and antigenicity (12, 21, 37). However, antibody against pVP2b did not neutralize infectivity or decorate particles by IEM. pVP2c was only weakly recognized by the rabbit anti-capsid antibody (Fig. 2A), none of the mink serum pools (Fig. 2B), and only 1 of 18 mink tested.

In summary, our results have indicated that selected portions of the ADV capsid proteins are important in the mink immune response to ADV. In particular, the noncontiguous sequences that likely constitute the threefold spike on the virion surface are major targets for antibody from infected animals and also contain neutralizing epitopes. Although antibody is unable to clear infectious virus from infected animals (40), antiviral antibody plays an important role in the immunopathogenesis by participating in immune complex generation (14, 41) and in the mediation of antibody-dependent infection of macrophage target cells (29). It will be interesting to determine if antibodies to the same regions of the virus are involved in all of these phenomena.

ACKNOWLEDGMENTS

The patience, assistance, and critical comments of Sylvia Perryman, Linda Dworak, Torben Storgaard, Robert Evans, Gary Hettrick, and Irene Rodriguez are gratefully acknowledged.

During the execution of these studies, D.A.M. and F.C. were Summer Intramural Research Training Associates of the National Institute of Allergy and Infectious Diseases. K.L.O. and M.H. were Special Volunteers employed by the Utah Fur Breeder's Agricultural Cooperative and the Mink Farmer's Research Foundation, respectively.

REFERENCES

1. **Aasted, B., and M. E. Bloom.** 1983. Sensitive radioimmune assay for measuring Aleutian disease virus and antibody. J. Clin. Microbiol. **18:**637–644.
2. **Aasted, B., and M. E. Bloom.** 1984. Mink with Aleutian disease have high affinity antiviral antibodies. Scand. J. Immunol. **19:**411–418.
3. **Aasted, B., G. S. Tierney, and M. E. Bloom.** 1984. Analysis of the quantity of antiviral antibodies from mink infected with different Aleutian disease virus strains. Scand. J. Immunol. **19:**395–402.
4. **Agbandje, M., R. McKenna, M. G. Rossmann, S. Kajigaya, and N. S. Young.** 1991. Preliminary X-ray crystallographic investigation of human parvovirus B19. Virology **184:**170–174.

5. **Agbandje, M., R. McKenna, M. G. Rossmann, M. L. Strassheim, and C. R. Parrish.** 1993. Structure determination of feline panleukopenia virus empty particles. Proteins **16:**1555–1571.
6. **Agbandje, M., C. R. Parrish, and M. G. Rossmann.** 1995. The structure of parvoviruses. Semin. Virol. **6:**299–309.
7. **Agbandje, M., C. R. Parrish, and M. G. Rossmann.** 1995. The recognition of parvovirus capsids by antibodies. Semin. Virol. **6:**219–231.
8. **Alexandersen, S., and B. Aasted.** 1986. Restricted heterogeneity of the early antibody response to Aleutian disease virus in mink kits. Acta Pathol. Microbiol. Immunol. Scand. Sect. C **94:**137–143.
9. **Alexandersen, S., M. E. Bloom, and S. Perryman.** 1988. Detailed transcription map of Aleutian mink disease parvovirus. J. Virol. **62:**3684–3694.
10. **Amann, E., J. Brosius, and M. Ptashne.** 1983. Vectors bearing a hybrid trp-lac promoter useful for regulated expression of cloned genes in Escherichia coli. Gene **25:**167–178.
11. **Bloom, M. E., S. Alexandersen, S. Perryman, D. Lechner, and J. B. Wolfinbarger.** 1988. Nucleotide sequence and genomic organization of Aleutian mink disease parvovirus (ADV): sequence comparisons between a nonpathogenic and a pathogenic strain of ADV. J. Virol. **62:**2903–2915.
12. **Bloom, M. E., B. D. Berry, W. Wei, S. Perryman, and J. B. Wolfinbarger.** 1993. Characterization of chimeric full-length molecular clones of Aleutian mink disease parvovirus (ADV): identification of a determinant governing replication of ADV in cell culture. J. Virol. **67:**5976–5988.
13. **Bloom, M. E., O.-R. Kaaden, E. Huggans, A. Cohn, and J. B. Wolfinbarger.** 1988. Molecular comparisons of in vivo and in vitro derived strains of Aleutian disease of mink parvovirus. J. Virol. **62:**132–138.
14. **Bloom, M. E., H. Kanno, S. Mori, and J. B. Wolfinbarger.** 1994. Aleutian mink disease: puzzles and paradigms. Infect. Agents Dis. **3:**279–301.
15. **Bloom, M. E., L. W. Mayer, and C. F. Garon.** 1983. Characterization of the Aleutian disease virus genome and its intracellular forms. J. Virol. **45:**977–984.
16. **Bloom, M. E., R. E. Race, W. J. Hadlow, and B. Chesebro.** 1975. Aleutian disease of mink: the antibody response of sapphire and pastel mink to Aleutian disease virus. J. Immunol. **115:**1034–1037.
17. **Bloom, M. E., R. E. Race, and J. B. Wolfinbarger.** 1980. Characterization of Aleutian disease virus as a parvovirus. J. Virol. **35:**836–843.
18. **Bloom, M. E., R. E. Race, and J. B. Wolfinbarger.** 1982. Identification of a nonvirion protein of Aleutian disease virus: mink with Aleutian disease have antibody to both virion and nonvirion proteins. J. Virol. **43:**608–616.
19. **Brown, C. S., T. Jensen, R. H. Meloen, W. Pujik, K. Sugamura, H. Sato, and W. J. M. Spaan.** 1992. Localization of an immunodominant domain on baculovirus-produced B19 capsids: correlation to a major surface region on the native virus particle. J. Virol. **66:**6989–6996.
20. **Chapman, M.** 1993. Mapping the surface properties of macromolecules. Protein Sci. **2:**459–469.
21. **Chapman, M. S., and M. G. Rossmann.** 1993. Structure, sequence and function correlates among parvoviruses. Virology **194:**491–508.
22. **Christensen, J., T. Storgaard, B. Bloch, S. Alexandersen, and B. Aasted.** 1993. Expression of Aleutian mink disease parvovirus proteins in a baculovirus vector system. J. Virol. **67:**229–238.
23. **Clemens, D. L., J. B. Wolfinbarger, S. Mori, B. D. Berry, S. F. Hayes, and M. E. Bloom.** 1992. Expression of Aleutian mink disease parvovirus capsid proteins by a recombinant vaccinia virus: self-assembly of capsid proteins into particles. J. Virol. **66:**3077–3085.
24. **Cotmore, S. F., and P. Tattersall.** 1987. The autonomously replicating parvoviruses. Adv. Virus Res. **33:**91–174.
25. **Crowe, J. S., H. J. Cooper, M. A. Smith, M. J. Sims, D. Parker, and D. Gewert.** 1991. Improved cloning efficiency of polymerase chain reaction (PCR) products after proteinase K digestion. Nucleic Acids Res. **19:**184.
26. **Gottschalk, E., S. Alexandersen, A. Cohn, L. Poulsen, M. E. Bloom, and B. Aasted.** 1991. Nucleotide sequence analysis of Aleutian mink disease parvovirus shows that multiple virus types are present in infected mink. J. Virol. **65:**4378–4386.
27. **Guan, C., P. Li, P. D. Riggs, and H. Inouye.** 1987. Vectors that facilitate the expression and purification of foreign peptides in *Escherichia coli* by fusion to maltose-binding protein. Gene **67:**21–30.
28. **Hadlow, W. J., R. E. Race, and R. C. Kennedy.** 1983. Comparative pathogenicity of four strains of Aleutian disease virus for pastel and sapphire mink. Infect. Immun. **41:**1016–1023.
29. **Kanno, H., J. B. Wolfinbarger, and M. E. Bloom.** 1993. Aleutian mink disease parvovirus infection of mink macrophages and human macrophage cell line U937: demonstration of antibody-dependent enhancement of infection. J. Virol. **67:**7017–7024.
30. **Kanno, H., J. B. Wolfinbarger, and M. E. Bloom.** 1993. Aleutian mink disease parvovirus infection of mink peritoneal macrophages and human macrophage cell lines. J. Virol. **67:**2075–2082.
31. **Langeveld, J. P. M., J. I. Casal, C. Vela, K. Dalsgaard, S. H. Smale, W. C. Pujik, and R. H. Meloen.** 1993. B-cell epitopes of canine parvovirus: distribution on the primary structure and exposure on the viral surface. J. Virol. **67:**765–772.
32. **Lee, S.-L., J. Stevens, W. W. Wang, and J. J. Lanzillo.** 1994. A liquid gelatin blocking reagent for western blotting with chemiluminescent detection. BioTechniques **17:**60–62.
33. **Lopez de Turiso, J. A., E. Cortes, A. I. Ranz, J. Garcia, A. Sanz, C. Vela, and J. I. Casal.** 1991. Fine mapping of canine parvovirus B cell epitopes. J. Gen. Virol. **72:**2445–2456.
34. **Maina, C., P. D. Riggs, A. G. Grandea, III, B. E. Slatko, L. S. Moran, J. A. Tagliante, L. A. McReynolds, and C. di Guan.** 1988. An Escherichia coli vector to express and purify foreign proteins by fusion to and separation from maltose-binding protein. Gene **74:**365–373.
35. **Oie, K. L., G. Durrant, J. B. Wolfinbarger, D. Martin, F. Costello, S. Perryman, W. J. Hadlow, and M. E. Bloom.** 1996. The relationship between capsid protein (VP2) sequence and pathogenicity of Aleutian mink disease parvovirus (ADV): a possible role for raccoons in the transmission of ADV infections. J. Virol. **70:**852–861.
36. **Oleksiewicz, M. B., F. Costello, M. Huhtanen, J. B. Wolfinbarger, S. Alexandersen, and M. E. Bloom.** 1996. Subcellular localization of Aleutian mink disease parvovirus proteins and DNA during permissive infection of Crandell feline kidney cells. J. Virol. **70:**3242–3247.
37. **Parrish, C. R., C. F. Aquadro, and L. E. Carmichael.** 1988. Canine host range and a specific epitope map along with variant sequences in the capsid protein gene of canine parvovirus and related feline, mink, and raccoon parvoviruses. Virology **166:**293–307.
38. **Porter, D. D.** 1986. Aleutian disease: a persistent parvovirus infection of mink with a maximal but ineffective host immune response. Prog. Med. Virol. **33:**42–60.
39. **Porter, D. D., F. J. Dixon, and A. E. Larsen.** 1965. Metabolism and function of gammaglobulin in Aleutian disease of mink. J. Exp. Med. **121:**889–900.
40. **Porter, D. D., and A. E. Larsen.** 1967. Aleutian disease of mink: infectious virus-antibody complexes in the serum. Proc. Soc. Exp. Biol. Med. **126:**680–682.
41. **Porter, D. D., A. E. Larsen, and H. G. Porter.** 1983. The pathogenesis of Aleutian disease of mink. III. Immune complex arteritis. Am. J. Pathol. **71:**331–344.
42. **Porter, D. D., H. G. Porter, A. E. Larsen, and M. E. Bloom.** 1987. Restricted viral antibody specificity in many ferrets infected with the ferret Aleutian disease parvovirus. Arch. Virol. **93:**155–161.
43. **Porter, D. D., H. G. Porter, S. C. Suffin, and A. E. Larsen.** 1984. Immunoglobulin classes of Aleutian disease virus antibody. Infect. Immun. **43:**463–466.
44. **Race, R. E., B. Chesebro, M. E. Bloom, B. Aasted, and J. Wolfinbarger.** 1986. Monoclonal antibodies against Aleutian disease virus distinguish virus strains and differentiate sites of virus replication from sites of viral antigen sequestration. J. Virol. **57:**285–293.
45. **Rimmelzwaan, G. F., J. Carlson, F. G. C. M. UytdeHaag, and A. D. M. E. Osterhaus.** 1990. A synthetic peptide derived from the amino acid sequence of canine parvovirus structural proteins which defines a B cell epitope and elicits antiviral antibody in BALB c mice. J. Gen. Virol. **71:**2741–2745.
46. **Rimmelzwaan, G. F., M. C. M. Poelen, R. H. Meloen, J. Carlson, F. G. C. M. UytdeHaag, and A. D. M. E. Osterhaus.** 1990. Delineation of canine parvovirus T cell epitopes with peripheral blood mononuclear cells and T cell clones from immunized dogs. J. Gen. Virol. **71:**2321–2329.
47. **Rosenfeld, S. J., K. Yoshimoto, S. Kajigaya, S. Anderson, N. S. Young, A. Field, P. Warrener, G. Bansal, and M. S. Collett.** 1992. Unique region of the minor capsid protein of human parvovirus B19 is exposed on the virion surface. J. Clin. Invest. **89:**2023–2029.
48. **Saiki, R. K., D. H. Gelfand, S. Stoffel, S. J. Scharf, R. Higuchi, G. T. Horn, K. B. Mullis, and H. A. Erlich.** 1988. Primer-directed enzymatic amplification of DNA with a thermostable DNA polymerase. Science **239:**487–491.
49. **Saravis, C. A.** 1984. Improved blocking of nonspecific antibody binding sites on nitrocellulose membranes. Electrophoresis **5:**54–55.
50. **Sato, H., J. Hirata, N. Kuroda, H. Shiraki, Y. Maeda, and K. Okochi.** 1991. Identification and mapping of neutralizing epitopes of human parvovirus B19 by using human antibodies. J. Virol. **65:**5485–5490.
51. **Schagger, H., H. Aquila, and G. Von Jagow.** 1988. Coomassie blue-sodium dodecyl sulfate-polyacrylamide gel electrophoresis for direct visualization of polypeptides during electrophoresis. Anal. Biochem. **173:**201–205.
52. **Shade, R. O., M. C. Blundell, S. F. Cotmore, P. Tattersall, and C. R. Astell.** 1986. Nucleotide sequence and genome organization of human parvovirus B19 isolated from the serum of a child during aplastic crisis. J. Virol. **58:** 921–936.
53. **Soderlund, M., K. E. Brown, O. Meurman, and K. Hedman.** 1992. Prokaryotic expression of a VP1 polypeptide antigen for diagnosis by a human parvovirus B19 antibody enzyme immunoassay. J. Clin. Microbiol. **30:**305–311.
54. **Stolze, B., and O.-R. Kaaden.** 1987. Apparent lack of neutralizing antibodies in Aleutian disease is due to masking of antigenic sites by phospholipids. Virology **158:**174–180.
55. **Strassheim, M. L., A. Gruenberg, P. M.-L. Veijalainen, J.-Y. Sgro, and C. R. Parrish.** 1994. Two dominant neutralizing antigenic determinants of canine parvovirus are found on the threefold spike of the virus capsid. Virology **198:**175–184.

56. **Thorpe, G. H. G., L. J. Kricka, S. B. Mosely, and T. P. Whitehead.** 1985. Phenols as enhancers of the chemiluminescent horseradish peroxidase-luminol-hydrogen peroxide reaction: application in luminescence-monitored enzyme immunoassays. Clin. Chem. **31:**1335–1341.
57. **Truyen, U., A. Gruenberg, S. F. Chang, B. Obermaier, P. M.-L. Veijalainen, and C. R. Parrish.** 1995. Evolution of the feline-subgroup parvoviruses and the control of canine host range in vivo. J. Virol. **69:**4702–4710.
58. **Tsao, J., M. S. Chapman, M. Agbandje, W. Keller, K. Smith, H. Wu, M. Luo, T. J. Smith, M. G. Rossmann, R. W. Compans, and C. R. Parrish.** 1991. The three-dimensional structure of canine parvovirus and its functional implications. Science **251:**1456–1464.
59. **Wu, W.-H., M. E. Bloom, B. D. Berry, M. J. McGinley, and K. B. Platt.** 1994. Expression of Aleutian mink disease parvovirus capsid proteins in a baculovirus expression system for potential diagnostic use. J. Vet. Diagn. Invest. **6:**23–29.
60. **Yanisch-Perron, C., J. Viera, and J. Messing.** 1985. Improved M13 phage cloning vectors and host strains: nucleotide sequences of the M13mp18 and pUC19 vectors. Gene **33:**103–119.